

# Effect of solution treatment on microstructure and mechanical properties of as-cast Al-12Si-4Cu-2Ni-0.8Mg-0.2Gd alloy

Yu-dong Sui<sup>1,2</sup>, Ye-hua Jiang<sup>1</sup>, and \*Qu-dong Wang<sup>2</sup>

1. School of Materials Science and Engineering, Kunming University of Science and Technology, Kunming 650093, China

2. National Engineering Research Center of Light Alloys Net Forming and State Key Laboratory of Metal Matrix Composite, Shanghai Jiao Tong University, Shanghai 200240, China

**Abstract:** Effect of solution treatment on microstructure and mechanical properties of Al-12Si-4Cu-2Ni-0.8Mg-0.2Gd alloy was investigated. Results show the Si particles become stable and more intermetallic compounds dissolve in the matrix after solution treatment at 500 °C for 2 h followed by 540 °C for 3 h (T4). The skeleton-like Al<sub>3</sub>CuNi develops into two parts in the T4 alloy: one is Al<sub>3</sub>CuNi which has the framework shape; the other is intermetallics including the Al<sub>3</sub>CuNi (size: 5–10 μm) and AlSiCuNiGd phases (size: ≤5 μm) with complex structure. Adding 0.2% Gd can improve the mechanical properties of the alloys after two-step solution treatment (500 °C/2 h followed by 540 °C/3 h), the hardness of the alloy increases from 130.9 HV to 135.8 HV compared with the alloy with one-step solution treatment (500 °C/2 h), the engineering strength increases from 335.45 MPa to 352.03 MPa and the fracture engineering strain increases from 1.44% to 1.67%.

**Keywords:** Al-Si-Cu-Ni-Mg alloy; Gd element; solution treatment; microstructure; mechanical properties

CLC numbers: TG146.21

Document code: A

## 1 Introduction

Al-Si alloys containing alloying elements, such as Cu, Mg and Ni, are utilized in the manufacturing of pistons to reduce the vehicle weight and improve the fuel efficiency, due to their good castability, low coefficient of thermal expansion, high strength-to-weight ratio and high room and elevated temperature strength<sup>[1–6]</sup>.

To further improve the mechanical properties of Al-Si-Cu-Ni-Mg alloys, heat treatment can be adopted. As a key step of heat treatment, the selection of solution parameters (such as temperature and time) is crucial. Suitable solution parameters can promote more alloying elements to dissolve into matrix, reduce vacancies, and spheroidize Si particles in Al-Si alloy. However, the incipient melting of phases is a strong obstacle to increase the solution treatment temperatures above the solidification temperature for Al-Si-Cu-Mg alloys<sup>[7]</sup>. If the solution treatment temperature exceeds the melting point of phases, localized melting at the grain boundaries

will occur and the mechanical properties of the alloy will be reduced<sup>[8]</sup>. To solve this problem, a two-step solution treatment can be used. A two-step solution treatment, namely, conventional solution treatment followed by a high temperature solution treatment, as suggested by Sokolowski et al.<sup>[9]</sup>, which significantly reduced the amount of the copper-rich phase in 319 alloys, thereby improved the mechanical properties of alloys. Azmah et al.<sup>[10]</sup> reported that the two-step solution treatment (495 °C/2 h followed by 515 °C/4 h) increased the hardness and tensile strength of the 332 alloy (Al-Si-Cu-Ni-Mg) significantly. They mainly concentrated on the incipient melting of Q-Al<sub>3</sub>Cu<sub>2</sub>Mg<sub>8</sub>Si<sub>6</sub>, θ-Al<sub>2</sub>Cu and M-Mg<sub>2</sub>Si phases and tried to dissolve more copper and magnesium containing intermetallics into the matrix, so as to improve the mechanical properties of the alloy. Samuel et al.<sup>[11]</sup> observed that a two-stage solution heat-treatment consisting of 12 h at 510 °C, followed by 12 h at 540 °C was a very effective heat-treatment for 319 alloys (Al-Si-Cu-Mg). The two-stage solution heat-treatment process has a twofold purpose: (a) the dissolution of copper-containing phases, mainly Al<sub>2</sub>Cu and Al<sub>5</sub>Mg<sub>8</sub>Cu<sub>2</sub>Si<sub>6</sub> at 510 °C, and (b) spheroidization of the eutectic silicon particles and dissolution of more intermetallics at higher temperatures.

Ni is recognized as the most effective element

\*Qu-dong Wang

Male, born in 1964, Ph. D, Professor. His research interests mainly focus on the light-weight materials.

E-mail: wangqudong@sjtu.edu.cn

Received: 2021-04-11; Accepted: 2021-08-11

in improving the mechanical properties of Al-Si-Cu-Ni-Mg alloys<sup>[12]</sup>. The  $\delta$ -Al<sub>3</sub>CuNi,  $\gamma$ -Al<sub>7</sub>Cu<sub>4</sub>Ni and  $\varepsilon$ -Al<sub>3</sub>Ni phases have great contributions to the mechanical properties of Al-Si multicomponent alloys, owing to their better thermal stability, mechanical properties, morphologies and distributions<sup>[13]</sup>. In our previous study<sup>[14]</sup>, the morphology of the AlSiFeNiCu aluminide and some Al<sub>3</sub>CuNi phases was changed from strip-like to small block-like after Gd added into the as-cast Al-12Si-4Cu-2Ni-0.8Mg piston alloy. And when the content of Gd was 0.2wt.%, the optimal elevated temperature ( $\geq 300$  °C) tensile strength was obtained. Nevertheless, little effort has focused on the evolution of Ni-rich phases and Gd-containing intermetallics during solution treatment and its impact on the mechanical properties of multicomponent Al-Si-Cu-Ni-Mg-Gd alloys.

The purpose of this work is to determine the optimum parameters of the solution treatments for Al-12Si-4Cu-2Ni-0.8Mg and Al-12Si-4Cu-2Ni-0.8Mg-0.2Gd alloys, and to study the influence of Gd on the evolution of the Al<sub>3</sub>CuNi phases during solution treatment.

## 2 Experimental details

The experimental alloys were prepared using 99.7% pure Al, 99.7% pure Mg, and Al-35%Si, Al-50%Cu, Al-10%Ni, Al-10%Mn and Mg-90%Gd master alloys. All compositions are given in wt.% hereafter, unless otherwise specified. The pure Al, pure Mg and Al-Si, Al-Cu, Al-Ni, Al-Mn master alloys were melted in an electric resistance furnace at  $730 \pm 5$  °C. After the alloy was melted completely, the Mg-Gd master alloy was added into the melt at 720 °C (this step is not required for Al-12Si-4Cu-2Ni-0.8Mg alloy). Then, the melt was isothermally held at 720 °C for about 30 min and stirred to guarantee a complete homogenization. Molten alloy was poured at 690 °C into a metallic mold preheated to 200 °C with the size of 130 mm (length)  $\times$  20 mm (width)  $\times$  110 mm (height). The chemical compositions of the alloy, determined by inductively coupled plasma-atomic emission spectrometry (ICP-AES), are listed in Table 1. Subsequently, JMatPro was applied to detect the possible intermetallic phases in Al-12Si-4Cu-2Ni-0.8Mg-0.2Gd alloy.

**Table 1: Chemical composition of experimental alloys (wt.%)**

Alloy	Si	Cu	Ni	Mg	Fe	Mn	Gd	Al
Al-12Si-4Cu-2Ni-0.8Mg	11.69	3.96	2.00	0.76	0.14	0.18	0	Bal.
Al-12Si-4Cu-2Ni-0.8Mg-0.2Gd	11.34	3.94	1.98	0.83	0.18	0.19	0.21	Bal.

Specimens were all sectioned at about 5 mm above the bottom surface of the as-cast samples. The following equation was used to estimate the homogenization time ( $t$ ) of the four major solute elements in the piston alloy<sup>[15]</sup>:

$$t \cong 0.3 \frac{\lambda^2}{D_s} \quad (1)$$

where  $\lambda$  is the secondary dendrite arm spacing, which is about 20  $\mu$ m for cast Al-12Si-4Cu-2Ni-0.8Mg alloy<sup>[16]</sup>, and  $D_s$  is the diffusivity of a given solute in aluminum at the temperatures specified in Table 2. Therefore, by substituting the above parameters into Eq. (1), it can be found that a solutionizing heat treatment at 500 °C (773 K) for 24 h is sufficient to achieve satisfactory homogenization. The traditional solution treatment of Al-12Si-4Cu-2Ni-0.8Mg alloy was 500 °C for 2 h to prevent incipient melting of  $\theta$ -Al<sub>2</sub>Cu and Q-Al<sub>5</sub>Cu<sub>2</sub>Mg<sub>8</sub>Si<sub>6</sub> phases. Therefore, some specimens were heat treated with a single-step solution treatment at 480, 500, 520, and 540 °C for 2, 3,

4, 6, 8, 12, and 24 h. Other samples were treated with a two-step solution treatment at 500 °C for 2 h followed by heating at 520 and 540 °C for another 2, 3, 4, 6, 8, 10, and 12 h. For both single-step and two-step solution treatment specimens, the quenching was carried out using boiled water between 70 °C and 90 °C.

Metallographic samples were mechanically ground and then polished in standard routines. The samples were etched using Keller etchant (5 mL HNO<sub>3</sub>, 3 mL HCl, 2 mL HF, and 190 mL distilled water) for 10 s. After etching, the microstructure was observed using an optical microscope (Axio Observer A1) and a scanning electron microscope (SEM 515) equipped with EDX. The ion-beam-milled TEM foils prepared using a Gatan Precision Ion Polishing System (PIPS, Gatan 691) were examined in a JEOL2100F-TEM at 200 kV. Measurements by differential scanning calorimetry (DSC) (STA 449 F3) were carried out on about 10 mg samples obtained from the alloys with different solution treatments under an argon atmosphere at a heating rate of 10 K·min<sup>-1</sup>. An empty alumina crucible was employed to improve the sensitivity of the DSC experiments. The volume fractions and morphologies of Si and Ni-containing phases were calculated and characterized using Image-Pro Plus software. Hardness tests were carried out on an HV-10 semi-automatic Vickers hardness tester. The load was 5 kg, the loading time was 20 s, and the hardness value was the average of 10 points. Tensile tests were performed at room temperature on a Zwick/Roell Z100 testing machine, using sheet specimens (ISO 6892-1:2009 standard<sup>[21]</sup>). To ascertain reproducibility, each test result was averaged from three tensile test specimens under identical conditions.

**Table 2: Estimate of homogenization times ( $t$ ) for four major solute elements in piston alloy**

Solute element	Diffusivity (m <sup>2</sup> ·s <sup>-1</sup> )	$t$ (h)	Refs.
Si	$0.64 \times 10^{-13}$ at 753 K	0.52	[17]
Cu	$1.54 \times 10^{-15}$ at 673 K	21.65	[18]
Ni	$0.84 \times 10^{-14}$ at 700 K	3.97	[19]
Mg	$1.61 \times 10^{-14}$ at 673 K	2.07	[20]

### 3 Results and discussion

#### 3.1 Precipitation sequence of phases

JMatPro calculation results are shown in Fig. 1. As can be seen from Fig. 1, there are three main intermetallics in the Al-12Si-4Cu-2Ni-0.8Mg-0.2Gd alloy. The precipitation sequence of these three intermetallics is  $\text{Al}_7\text{Cu}_4\text{Ni}$ ,  $\text{Al}_3\text{CuNi}$ , and  $\text{Al}_5\text{Cu}_2\text{Mg}_8\text{Si}_6$ . The DSC curves of the Al-12Si-4Cu-2Ni-0.8Mg-0.2Gd alloys with different solution treatments are shown in Fig. 2. Belov et al. [22], Yang et al. [23] and Zeren et al. [24] have conducted the research on the solidification of the Al-Si-Cu-Ni-Mg system in detail. Their results show that many intermetallics (such as  $\text{Al}_5\text{Cu}_2\text{Mg}_8\text{Si}_6$ ,  $\text{Al}_3\text{CuNi}$ ,  $\text{Al}_7\text{Cu}_4\text{Ni}$ , etc.) are formed after solidification of Al-Si-Cu-Ni-Mg alloy. In our work, the DSC curves of alloy exhibits a very small endothermic peak at 494 °C, labeled as Point 1, corresponding to the formation of  $\text{Q-Al}_5\text{Cu}_2\text{Mg}_8\text{Si}_6$  phases. The Point 2 at 502 °C, corresponding to the formation of  $\theta\text{-Al}_2\text{Cu}$  phases.

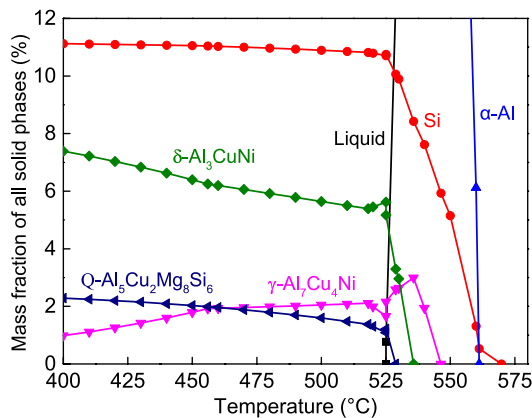


Fig. 1: JMatPro calculation of possible intermetallic phases in Al-12Si-4Cu-2Ni-0.8Mg-0.2Gd alloy

Subsequently, the Point 3 at 513 °C, corresponding to the formation of  $\gamma\text{-Al}_7\text{Cu}_4\text{Ni}$  phases. The Point 4 at 527 °C and Point 5 at 537 °C correspond to the formation of  $\delta\text{-Al}_3\text{CuNi}$  and  $\varepsilon\text{-Al}_3\text{Ni}$  phases, respectively. The formation of Gd-containing phases cannot be detected from DSC curve due to too low the content. From the DSC results, it can be seen that Points 1 and 2 disappear after single-step solution treatment (500 °C/2 h), and Points 4 and 5 is not obvious after two-step solution treatment (500 °C/2 h+540 °C/3 h).

#### 3.2 Microstructures of specimens

The typical microstructures of Al-12Si-4Cu-2Ni-0.8Mg-0.2Gd under different solution treatments are shown in Figs. 3.  $\alpha\text{-Al}$  matrix, different morphologies of Si particles and intermetallic phases can be found in the alloys. The solution treatments were found have effect on the morphology of the Si particles and the volume fraction of intermetallics. The edges of the Si particles become more round and some intermetallics disappear with the

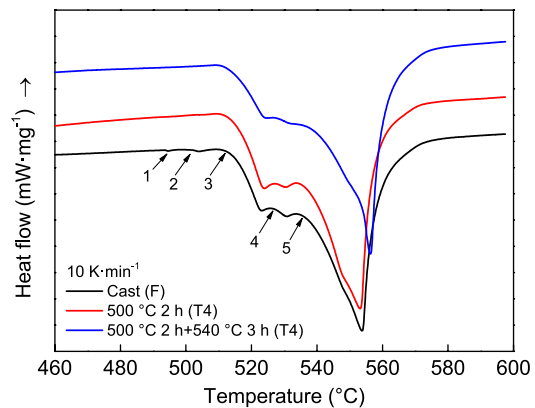


Fig. 2: DSC curves of Al-12Si-4Cu-2Ni-0.8Mg-0.2Gd alloy with different solution treatments

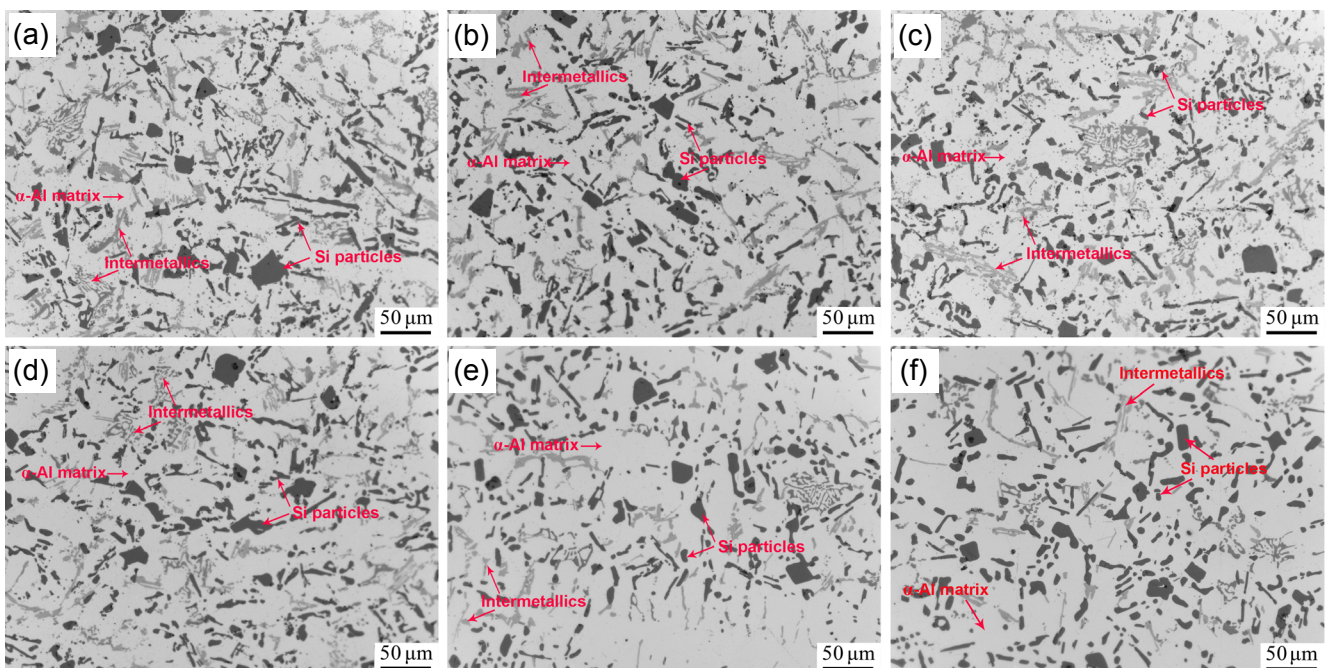


Fig. 3: Light optical micrographs of Al-12Si-4Cu-2Ni-0.8Mg-0.2Gd alloy with a two-step solution treatment at 500 °C/2 h followed by 520 °C/2 h (a); 520 °C/4 h (b); 520 °C/10 h (c); 540 °C/2 h (d); 540 °C/3 h (e); 540 °C/10 h (f)



increase of solution temperature and solution time.

Eight types of phases including primary  $\alpha$ -Al, primary Si, eutectic Si, AlSiFeNiCu-aluminide, Q-Al<sub>3</sub>Cu<sub>2</sub>Mg<sub>8</sub>Si<sub>6</sub>,  $\theta$ -Al<sub>2</sub>Cu,  $\gamma$ -Al<sub>7</sub>Cu<sub>4</sub>Ni and  $\delta$ -Al<sub>3</sub>CuNi were detected in the as-cast Al-12Si-4Cu-2Ni-0.8Mg alloy<sup>[15]</sup> [Fig. 4(a)]. It can be observed in Fig. 4(b) that  $\theta$ -Al<sub>2</sub>Cu and some Q-Al<sub>3</sub>Cu<sub>2</sub>Mg<sub>8</sub>Si<sub>6</sub> phases are dissolved into the matrix after the conventional solution heat treatment (500 °C/2 h). After the two-step heat treatment (500 °C/2 h+540 °C/3 h), as shown in Fig. 4(c), it is difficult to identify the undissolved  $\gamma$ -Al<sub>7</sub>Cu<sub>4</sub>Ni phases. However, some Q-Al<sub>3</sub>Cu<sub>2</sub>Mg<sub>8</sub>Si<sub>6</sub> phases still remain in the matrix due to the limited solubility of Cu in Al. The edges of these residual Q phases are significantly blunted.

The SEM images of Al-12Si-4Cu-2Ni-0.8Mg and Al-12Si-

4Cu-2Ni-0.8Mg-0.2Gd alloys after 500 °C/2 h+540 °C/3 h solution treatment are shown in Fig. 5. The phases are labeled and their compositions are given in Table 3. As shown in Fig. 5(a), the Al<sub>3</sub>CuNi phase (Label 1) exhibits white skeleton-like morphology in the Al-12Si-4Cu-2Ni-0.8Mg alloy. However, the skeleton-like Al<sub>3</sub>CuNi develops into two parts in the Al-12Si-4Cu-2Ni-0.8Mg-0.2Gd alloy: one is Al<sub>3</sub>CuNi in framework shape (Label 3); the other is broken intermetallics which include Al<sub>3</sub>CuNi (Label 4, size: 5–10  $\mu$ m) and Gd-containing (Label 2 and 5, size:  $\leq$ 5  $\mu$ m) phases.

The TEM characterization combined with EDX analysis of the Al<sub>3</sub>CuNi and Gd-containing phases are shown in Fig. 6. The phases are labeled and identified in the TEM graphs and their compositions are given in Table 4. The chemical composition of

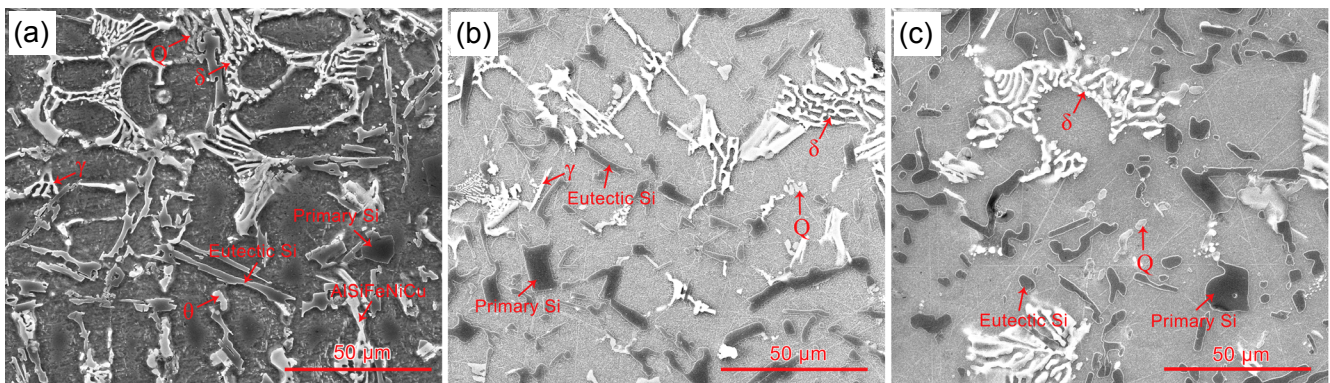


Fig. 4: Microstructure of Al-12Si-4Cu-2Ni-0.8Mg alloy at different solution treatments: (a) as-cast condition; (b) 500 °C/2 h; (c) 500 °C/2 h+540 °C/3 h

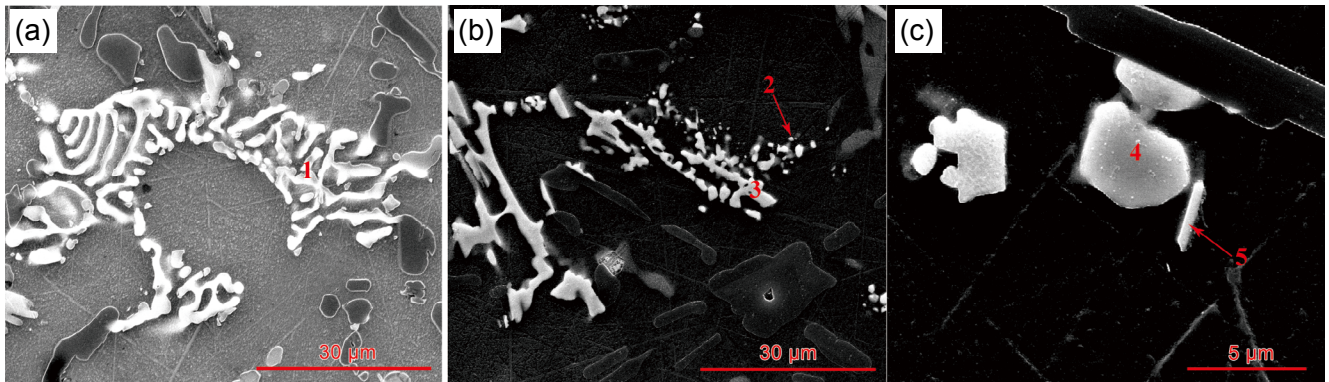


Fig. 5: SEM images of Al-12Si-4Cu-2Ni-0.8Mg (a) and Al-Si-Cu-Ni-Mg-Gd (b and c) alloys after 500 °C/2 h+540 °C/3 h solution treatment

Table 3: Compositions of phases in Fig. 5 by EDS

Number	Element (at.%)							Phase
	Al	Si	Cu	Mg	Ni	Fe	Gd	
1	68.21	-	15.14	-	16.13	0.53	-	Al <sub>3</sub> CuNi
2	62.24	8.87	9.63	1.21	15.21	0.81	2.04	Gd-containing
3	67.93	0.49	13.08	-	18.14	0.37	-	Al <sub>3</sub> CuNi
4	64.22	0.54	15.48	-	19.15	0.61	-	Al <sub>3</sub> CuNi
5	79.61	6.85	2.59	1.08	8.29	0.47	1.11	Gd-containing

the Phase A corresponds to  $\text{Al}_3\text{CuNi}$  phase with hexagonal crystal structure. The chemical composition of the Gd-containing phase (marked B) corresponds to  $\text{AlSiCuNiGd}$  phase with complex crystal structure, which has not been reported before. Combined with Fig. 5 and Table 3, the difference between the morphology of  $\text{AlSiCuNiGd}$  phase and  $\text{Al}_3\text{CuNi}$  phase of  $\text{Al-12Si-4Cu-2Ni-}$

$0.8\text{Mg-0.2Gd}$  alloy after two-step solution treatment is explained as follows: one reason is that the electronegativity differences between Gd and Al or Ni are greater than those between Cu and Al or Ni. Another reason might be that Gd decreases the diffusion rates of Cu and Ni in the solution treatment process and the intermetallics might not be coarsened during heat treatment<sup>[25]</sup>.

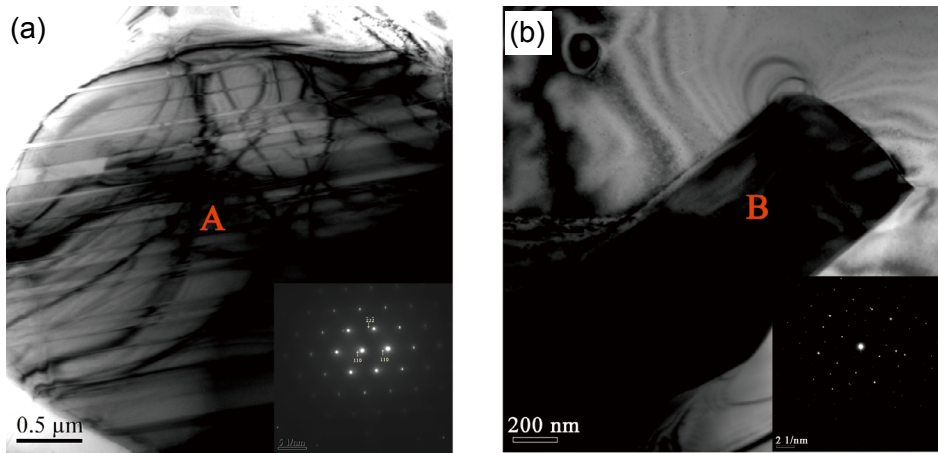


Fig. 6: TEM bright-field image and selected area electron diffraction (SAED) patterns of phases: (a)  $\text{Al}_3\text{CuNi}$ ; (b)  $\text{AlSiCuNiGd}$  phases

Table 4: EDX results of Points A and B in Fig. 6

Element	Point A		Point B	
	wt.%	at.%	wt.%	at.%
Al	55.15	73.61	21.92	40.38
Si	-	-	4.72	8.36
Cu	26.11	14.80	13.98	10.93
Ni	17.33	10.63	37.59	31.81
Fe	1.41	0.96	2.86	2.54
Gd	-	-	18.93	5.98
Totals	100.00	100.00	100.00	100.00

### 3.3 Morphological characteristics of phases

Mechanical properties of cast Al-Si alloys are greatly dependent on the size, morphology and distribution of Si particles and intermetallics. Figure 7 presents the Si particles' characteristics and the volume fraction of Ni-containing phases in  $\text{Al-12Si-4Cu-2Ni-0.8Mg-0.2Gd}$  alloy as function of solution temperature and time. At least 20 OM pictures were measured to provide reasonable statistical results. As can be seen in Figs. 7(a) and (b), the primary Si and eutectic Si phases become rounder after both the single-step and two-step solution treatment and the effect is more pronounced for samples treated with the single-step treatment at  $540\text{ }^{\circ}\text{C}$  for more than 2 h or two-step treatment at  $500\text{ }^{\circ}\text{C}$  for 2 h followed by  $540\text{ }^{\circ}\text{C}$  for more than 4 h. It is well known that the needle-like eutectic Si phases act as stress concentrator to reduce the strength of the material. The spherical morphology of the Si phases is expected to improve the mechanical properties of

the alloys. As shown in Fig. 7, the Si particles' characteristics become stable and more Ni-containing compounds dissolve in the matrix after the solution treatment at  $500\text{ }^{\circ}\text{C}$  for 2 h followed by  $540\text{ }^{\circ}\text{C}$  for 3 h.

### 3.4 Mechanical properties

The hardness test results of the  $\text{Al-12Si-4Cu-2Ni-0.8Mg-0.2Gd}$  alloy after single-step and two-step solution treatments are shown in Fig. 8. Comparing the change rules of the six hardness curves, it can be seen that the hardness of the alloy firstly increases and then decreases in both single-step solution and two-step solution. Due to the addition of 0.2% Gd in the alloy, the lattice distortion is produced, and the solution strengthening effect is enhanced, which makes the hardness of the alloy increase in the early solution stage. At the same time, Gd element also promotes the precipitation of the high melting point hard rare earth phase, thereby increasing the peak hardness value of the alloy (the peak aging hardness of  $\text{Al-12Si-4Cu-2Ni-0.8Mg}$  is about 128 HV)<sup>[26]</sup>. Under single-step solution conditions, when the solution temperature is no less than  $520\text{ }^{\circ}\text{C}$ , the higher the solution temperature, the faster the hardness rises. The hardness of the alloys reaches the maximum after about 2 h. It indicates that in this temperature range, the higher the solution temperature, the more the intermetallic compounds dissolves into the matrix, and the better the solution strengthening effect. However, an excessively high solution temperature will cause overburning of the low melting point precipitated phase and coarsening of the grain, resulting in a decrease in the hardness of the alloy. Under the two-step solution condition, the solution treatment has a better effect on improving the peak hardness. When the solution condition is  $500\text{ }^{\circ}\text{C}/2\text{ h}+540\text{ }^{\circ}\text{C}/3\text{ h}$ , the hardness of the alloy reaches the maximum value of 135.8 HV. For two-step

solution treatment alloy, during the first step of low temperature solution, the low melting point phases dissolve into matrix and solute atoms cause lattice distortion, the undissolved high melting point compounds are partially dissolved in the high temperature of the second step, causing further increase in hardness.

The engineering stress-strain tensile curves in as-cast and solution heat treated samples are plotted in Fig. 9. Compared with untreated alloy, the engineering stress and strain of Al-12Si-4Cu-2Ni-0.8Mg alloy treated by single-step solution increase about 48.3% and 75.3%, while those of the alloy treated by two-step solution treatment increase about 55.7% and 97.3%, respectively. The round morphology of the silicon phases can reduce the stress concentration at particle-matrix interfaces, improving the mechanical properties of alloys. Furthermore, Cu,

Mg and Ni alloying elements, which dissolved into  $\alpha$ -Al matrix, can contribute to the further enhanced mechanical properties of the tested alloy [27]. As can be seen in Fig. 9, adding 0.2% Gd to Al-12Si-4Cu-2Ni-0.8Mg alloy can improve its mechanical properties after two-step solution treatment, the engineering strength increases from 335.45 MPa to 352.03 MPa and the fracture engineering strain from 1.44% to 1.67%.

Analysis above shows that flake-like Si particles and skeleton-like  $\text{Al}_3\text{CuNi}$  are bad for the tensile properties of the Al-Si alloy, while spheroid-like Si particles and fine  $\text{AlSiCuNiGd}$  phases present positive effect. It is because that flake-like phase is easy to lead to the generation of crack, while the fine spheroid-like phases have a lower tendency to form cracks [27]. After the addition of Gd,  $\text{AlSiCuNiGd}$  phases with favorable morphology

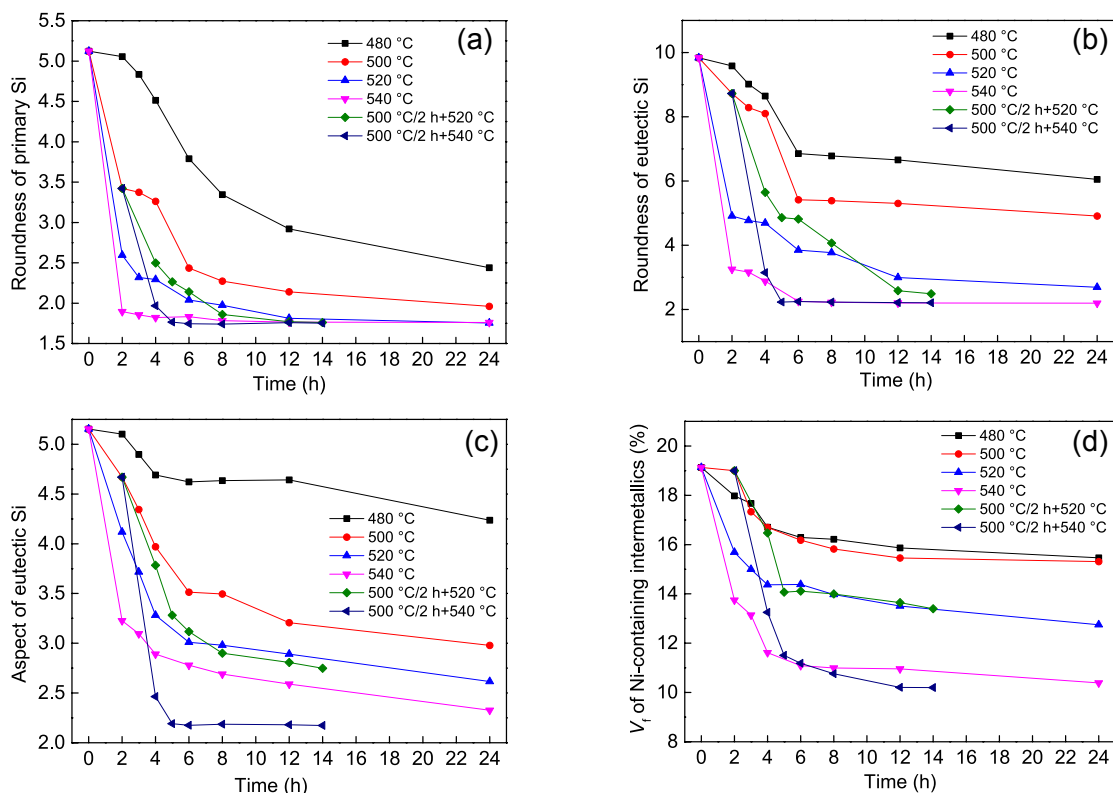


Fig. 7: Quantitative metallographic parameters of phases in Al-12Si-4Cu-2Ni-0.8Mg-0.2Gd alloy as function of solution temperature and time: (a) roundness of primary Si; (b) roundness of eutectic Si; (c) aspect of eutectic Si; (d) volume fraction ( $V_f$ ) of intermetallic phases in matrix

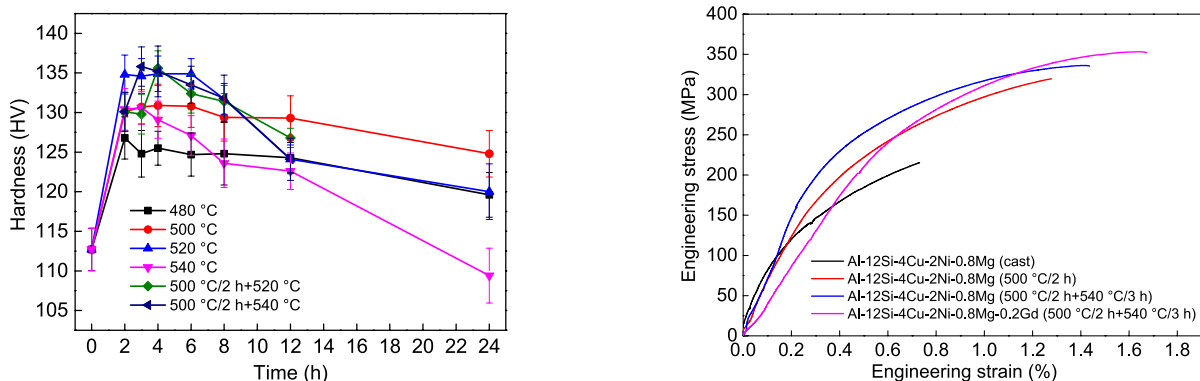


Fig. 8: Hardness curves of cast Al-12Si-4Cu-2Ni-0.8Mg-0.2Gd alloy at different solution temperatures and solution times

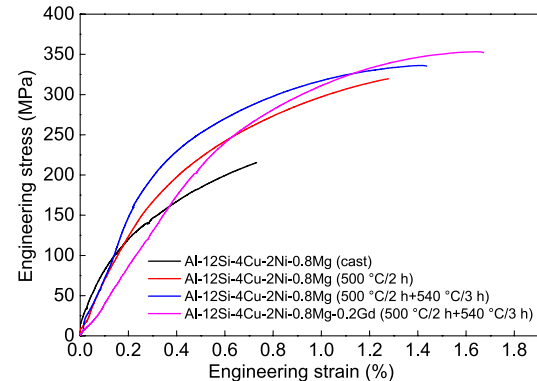


Fig. 9: Engineering compressive stress-strain curves at room temperature after different solution treatments



form and disperse evenly in Al matrix, as shown in Fig. 5. The single-step and two-step solution treatments successfully spheroidize and refine the silicon phases and help to increase the strength of the Al-12Si-4Cu-2Ni-0.8Mg alloy.

## 4 Conclusions

The effect of Gd and solution treatment on microstructure and mechanical properties of Al-12Si-4Cu-2Ni-0.8Mg alloy was investigated. The following conclusions can be drawn:

(1) The skeleton-like  $\text{Al}_3\text{CuNi}$  develops into two parts in solution treated Al-12Si-4Cu-2Ni-0.8Mg-0.2Gd alloy: one is  $\text{Al}_3\text{CuNi}$  which in framework shape; the other is broken intermetallics which include  $\text{Al}_3\text{CuNi}$  (size: 5–10  $\mu\text{m}$ ) and  $\text{AlSiCuNiGd}$  phases (size:  $\leq 5 \mu\text{m}$ ) with complex crystal structure.

(2) Al-12Si-4Cu-2Ni-0.8Mg-0.2Gd alloy treated by two-step solution (500 °C/2 h followed by 540 °C/3 h) has a higher peak hardness value than that treated by single-step solution (500 °C/2 h), which increases from 130.9 HV to 135.8 HV.

(3) Compared with untreated alloy, the engineering strength and fracture strain of Al-12Si-4Cu-2Ni-0.8Mg alloy treated by two-step solution treatment increase about 55.7% and 97.3%, respectively.

(4) Adding 0.2% Gd to the Al-12Si-4Cu-2Ni-0.8Mg alloy can improve mechanical properties after two-step solution treatment. The engineering strength increases from 335.45 MPa to 352.03 MPa and the fracture engineering strain from 1.44% to 1.67%.

## Acknowledgements

This work was financially supported by the National Natural Science Foundation of China (No. U1902220) and Yunnan Fundamental Research Projects (No. 202101BE070001-041).

## References

- [1] Hirsch J, Al-Samman T. Superior light metals by texture engineering: Optimized aluminum and magnesium alloys for automotive applications. *Acta Mater.*, 2013, 61(3): 818–843.
- [2] Manasijevic S, Radisa R, Markovic S, et al. Thermal analysis and microscopic characterization of the piston alloy  $\text{AlSi}_{13}\text{Cu}_4\text{Ni}_2\text{Mg}$ . *Intermetallics*, 2011, 19(4): 486–492.
- [3] Fernández G R, Requena G C. The effect of spheroidization heat treatment on the creep resistance of a cast  $\text{AlSi}_{12}\text{CuMgNi}$  piston alloy. *Mater. Sci. and Eng. A*, 2014, 598: 147–153.
- [4] Schöbel M, Baumgartner G, Gerth S, et al. Microstresses and crack formation in  $\text{AlSi}_7\text{MgCu}$  and  $\text{AlSi}_{17}\text{Cu}_4$  alloys for engine components. *Acta Mater.*, 2014, 81: 401–408.
- [5] Lu S P, Du R, Liu J P, et al. A new fast heat treatment process for cast A356 alloy motorcycle wheel hubs. *China Foundry*, 2018, 15(1): 11–16.
- [6] Dang B, Jian Z Y, Xu J F, et al. Effect of phosphorus and heat treatment on microstructure of Al-25%Si alloy. *China Foundry*, 2017, 14(1): 10–15.
- [7] Aguilera L I, Mancha M H, Castro Román M J, et al. Improvement of the tensile properties of an Al-Si-Cu-Mg aluminum industrial alloy by using multi stage solution heat treatments. *Mater. Sci. and Eng. A*, 2013, 561: 1–6.
- [8] Samuel F H. Incipient melting of  $\text{Al}_3\text{Mg}_8\text{Si}_6\text{Cu}_2$  and  $\text{Al}_2\text{Cu}$  intermetallics in unmodified and strontium-modified Al-Si-Cu-Mg (319) alloys during solution heat treatment. *J. Mater. Sci.*, 1998, 33: 2283–2297.
- [9] Sokolowski J H, Kierkus C A, Northwood D O. Improvement of 319 aluminum alloy casting durability by high temperature solution treatment. *J. Mater. Process. Technol.*, 2001, 109: 174–180.
- [10] Azmah H M A, Chang C S, Khang C O. Effect of a two-step solution heat treatment on the microstructure and mechanical properties of 332 aluminium silicon cast alloy. *Mater. Des.*, 2011, 32: 2334–2338.
- [11] Sablonniere H, Famuel F H. Solution heat-treatment of 319 aluminum alloy containing ~0.5wt.% Mg, Part 2: Microstructure and fractography. *Int. J. Cast Met. Res.*, 1996, 9: 151–225.
- [12] Joyce M R, Styles C M, Reed P A S. Elevated temperature short crack fatigue behaviour in near eutectic Al-Si alloys. *Int. J. Fatigue*, 2003, 25: 863–869.
- [13] Li Y G, Yang Y, Wu Y Y, et al. Quantitative comparison of three Ni-containing phases to the elevated-temperature properties of Al-Si piston alloys. *Mater. Sci. and Eng. A*, 2010, 527: 7132–7137.
- [14] Sui Y D, Wang Q D, Liu T, et al. Influence of Gd content on microstructure and mechanical properties of cast Al-12Si-4Cu-2Ni-0.8Mg alloys. *J. Alloys Compd.*, 2015, 644: 228–235.
- [15] Biswas A, Siegel D J, Seidman D N. Compositional evolution of Q-phase precipitates in an aluminum alloy. *Acta Mater.*, 2014, 75: 322–336.
- [16] Sui Y D, Wang Q D, Wang G L, et al. Effects of Sr content on the microstructure and mechanical properties of cast Al-12Si-4Cu-2Ni-0.8Mg alloys. *J. Alloys Compd.*, 2015, 622: 572–579.
- [17] Fujikawa S, Hirano K, Fukushima Y. Diffusion of silicon in aluminum. *Metall. Trans. A*, 1978, 9: 1911–1815.
- [18] Knipling K E, Dunand D C, Seidman D N. Criteria for developing castable, creep-resistant aluminum-based alloys – A review. *Z. Metallkd.*, 2006, 97: 246–265.
- [19] Eremenko V N, Natanzon Y V, Titov V P. Dissolution kinetics and diffusion coefficients of iron, cobalt, and nickel in molten aluminum. *Mater. Sci.*, 1978, 14: 579–584.
- [20] Fujikawa S, Takada Y. Interdiffusion between aluminum and Al-Mg alloys. *Defect and Diffusion Forum*, 1997, 143–147: 409–414.
- [21] ISO 6892-1:2009. Metallic materials-Tensile testing-Part 1: Method of test at room temperature. ISO 2009.
- [22] Belov N A, Eskin D G, Avxentieva N. Constituent phase diagrams of the Al-Cu-Fe-Mg-Ni-Si system and their application to the analysis of aluminium piston alloys. *Acta Mater.*, 2005, 53(17): 4709–4722.
- [23] Yang Y, Yu K L, Li Y G, et al. Evolution of nickel-rich phases in Al-Si-Cu-Ni-Mg piston alloys with different Cu additions. *Mater. Des.*, 2012, 33: 220–225.
- [24] Zeren M. The effect of heat-treatment on aluminum-based piston alloys. *Mater. Des.*, 2007, 28(9): 2511–2517.
- [25] Li Y G, Wu Y Y, Qian Z, et al. Effect of co-addition of RE, Fe and Mn on the microstructure and performance of A390 alloy. *Mater. Sci. and Eng. A*, 2009, 527(1–2): 146–149.
- [26] Abdulwahab M, Madugu I A, Yaro S A, et al. Effects of multiple-step thermal ageing treatment on the hardness characteristics of A356.0-type Al-Si-Mg alloy. *Mater. Des.*, 2011, 32: 1159–1166.
- [27] Mohamed A M A, Samuel A M, Samuel F H, et al. Influence of additives on the microstructure and tensile properties of near-eutectic Al-10.8%Si cast alloy. *Mater. Des.*, 2009, 30: 3943–3957.